A coupling model for cooperative dynamics in shape memory polymer undergoing multiple glass transitions and complex stress relaxations

Xiaodong Wang[a], Yuheng Liu[a], Haibao Lu[a,*] Nan Wu[b], David Hui[c] and Yong-Qing Fu[d]

[a]Science and Technology on Advanced Composites in Special Environments Laboratory, Harbin Institute of Technology, Harbin 150080, China

[b]Department of Mechanical Engineering, University of Manitoba, Winnipeg, Manitoba, R3T 2N2, Canada

[c]Composite Material Research Laboratory, Department of Mechanical Engineering, University of New Orleans, LA 70148, USA

[d]Faculty of Engineering and Environment, Northumbria University, Newcastle upon Tyne, NE1 8ST, UK

[*]Corresponding author, E-mail: luhb@hit.edu.cn

ABSTRACT: Modelling multi-shape memory effect (multi-SME) of shape memory polymers (SMPs) is a critical challenge for fields of engineering, mathematics/statistics and condensed-matter physics. These SMPs have a huge number of segments and their thermomechanical behaviors are determined by heating methods/history and cooperative relaxations (e.g., relaxation of all segments occurs simultaneously). In this study, a one-dimensional coupling model was proposed to investigate the cooperative dynamics of multiple glass transitions and thermomechanical behaviors of the SMPs. The overall relaxation behaviors of different tangled segments in the SMPs were formulated based on the Boltzmann's superposition principle by coupling the highest

transition temperature (T_{max}) and initial transition temperature (T_{min}) of all segments. Dependences of thermomechanical properties and relaxation strains upon the parameters of T_{max}, T_{min}, relaxation time and heating rate were theoretically investigated. Multiple glass transitions, thermomechanical and shape memory behaviors of the SMPs have been well described using this newly proposed coupling model. Finally, the simulation results were compared with the experimental data, and good agreements between them were obtained.

Keywords: shape memory polymer; shape memory effect; cooperative dynamics

1. Introduction

Shape memory polymer (SMP) is classified as a stimulus-responsive material which, after a pre-deformation, has the superior ability of memorizing and regaining its original shape [1]. In microscale, there are many segments tangled each other inside the SMP, which generate reversibly configurational entropy and enable the macromolecule chains having the shape memory effect (SME). SMPs have attracted a lot of attention because of their sensitivities to temperature and other stimuli such as light, electricity and chemicals [2-5]. Various types of SMPs including electrically/magnetically actuated ones and light/chemically responsive ones [2-5] have been developed in recent years. Their properties have been investigated and tested extensively for a wide range of applications, from aerospace engineering to biomedicine [6-9].

Over the last few years, there has also been a great interest in the development of SMPs with multi-SME [10], which is originated from the multiple glass transitions [11,12] and structural relaxation in the SMP [13-16]. When macromolecules of the

SMP are incorporated with one hard segment and more than two soft segments, multi-SME could be generated through the reversibly configurational entropy of all soft segments under an appropriate stimulus [10]. As is well known, an appropriate transition temperature difference between two adjacent soft segments is necessary to present a distinct multi-SME [13]. Otherwise, the transition behaviors of two processes will be overlapped due to their cooperative transitions (e.g., transitions of all segments occur simultaneously). This is to say that the highest transition temperature (T_{max}, defined as the finish temperature of phase transition) of the first soft segment should be lower than the initial transition temperature (T_{min}, defined as the starting temperature of phase transition) of the second soft segment. Several important parameters such as transition temperature, relaxation time, heating rate and thermomechanical modulus play critical roles in determining the multi-SME [17-21]. In terms of thermodynamics, multi-shape memory behavior is originated from the segmental relaxation of multiple segments, which then respond in a time and temperature dependent manner [22,23]. Therefore, phase/state transition and stress relaxation are the driving force of the multi-SME and shape memory behavior, respectively [24,25].

In the previous studies, the constitutive relations are typically investigated using a specific modeling frame of either glass transition temperature (T_g) or relaxation time [11,21,24]. Therefore, extended Maxwell models with multiple non-equilibrium equations have been employed to explain the complicated thermomechanical and shape memory behaviors of SMPs [22-24]. These models are expected to describe the constitutive relationships of the SMPs, which are critical for discovery of new material

[26,27] and engineering structural design [28,29]. However, these phenomenological studies need huge effort of calculations to determine parameters of the models and then to be verified by means of experimental measurements.

In this study, we propose a coupling model to explore the cooperative dynamics in multi-SME of the SMP undergoing multiple glass transitions. Boltzmann's superposition principle is initially introduced to characterize the overall coupling interactions and relaxation behavior of all the segments [24]. Dependences of thermomechanical properties and relaxation strains on the temperature, relaxation time and heating rate were then theoretically investigated using this newly proposed model. Finally, the simulation results were compared with the experimental data reported inliterature [23,30,31] for further verifications. In this study, the one-dimensional coupling model was proposed to explore the cooperative dynamics of multiple glass transitions and the thermomechanical behaviors of the SMPs. The studies of 3D and large deformation of SMPs without multi-SME have previously been investigated and reported in literature [28,32,33].

2. Constitutive model

According to the previously reported phenomenological method [15], it is assumed that the SME in SMPs is originated from the transition of soft segments from their frozen phases into active ones with an increase in temperature. The function ϕ_f is introduced as the volume fraction of the frozen phase in the soft segment. When ϕ_f =1, it implies that there is no transition. While if ϕ_f =0, a 100% transition is assumed

to be achieved and the soft segment is in the active phase. It is assumed that the frozen and active phases are in series connections and contributed to the thermomechanical behavior of SMP. Therefore, the series connection model of various soft segments has been used to characterize the multi-SME and predict the shape memory behaviors [34,35].

A normalized strain λ^i ($\sum_{i=1}^{n}\lambda^i=1$, $1\le i\le n$) is used to represent the strain ratio of the *i*th soft segment in the whole macromolecules. The constitutive relationship among the functions of ϕ_f^i, $T_{\max}^i$ and $T_{\min}^i$ for the *i*th soft segment of the SMP can be described as follows [19]:

$$\phi_f^i(T)=\left(1-\left(\frac{T-T_{\min}^i}{T_{\max}^i-T_{\min}^i}\right)^{m^i}\right)^{n^i}\quad(T_{\min}^i\le T\le T_{\max}^i) \tag{1}$$

where m^i and n^i are two given constants. $\phi_f^i(T_{\min}^i)=1$ and $\phi_f^i(T_{\max}^i)=0$.

According to the one-parameter model [36], the $T_{\max}^i$ is determined by the heating rate and has a relationship as below:

$$T_{\max}^i=B^i\ln q+A^i \tag{2}$$

where q is the heating rate, A^i and B^i are the given constants.

Substituting Equation (2) into Equation (1), we can obtain:

$$\phi_f^i(T)=\left(1-\left(\frac{T-T_{\min}^i}{B^i\ln q+A^i-T_{\min}^i}\right)^{m^i}\right)^{n^i}\quad(T_{\min}^i\le T\le T_{\max}^i) \tag{3}$$

Therefore, the volume fraction of the active phase ($\phi_a^i(T)$) can be obtained,

$$\phi_a^i(T)=1-\phi_f^i(T)=1-\left(1-\left(\frac{T-T_{\min}^i}{B^i\ln q+A^i-T_{\min}^i}\right)^{m^i}\right)^{n^i} \tag{4}$$

If the heating rates applied on the soft segment are different, the volume fraction of frozen phase can be further written as:

$$\phi_f^i(T) = 1 - \sum_{k=1}^{z} \{ \left[\phi_a^i(T_k) - \phi_a^i(T_{k-1}) \right] \Big|_{q_k} \} \tag{5}$$

where T_0 is the initial temperature, $\phi_a^i(T_k)$ and $\phi_a^i(T_{k-1})$ are the volume fractions of active phases at the temperatures of T_k and T_{k-1} at a heating rate of q_k, respectively, and z represents the numbers of heating rates.

On the other hand, the strain ($\varepsilon^i(T)$) applied onto the soft segment in SMPs is determined by the volume fraction of frozen phase based on Liu et al's model [15],

$$\varepsilon^i(T) = \phi_f^i(T) \varepsilon_{pre}^i \tag{6}$$

where ε_{pre}^i is the pre-stored strain in the *i*th soft segment.

Based on the Boltzmann's superposition principle [24], the overall stored strain ($\varepsilon(T)$) with respect to $\phi_f^i(T)$ can be described using:

$$\varepsilon(T) = \sum_{i=1}^{n} \phi_f^i(T) \varepsilon_{pre}^i = \sum_{i=1}^{n} \left(1 - \left(\frac{T - T_{\min}^i}{B^i \ln q + A^i - T_{\min}^i} \right)^{m^i} \right)^{n^i} \varepsilon_{pre}^i \tag{7}$$

where n is the total number of soft segments in the SMP.

On the other hand, the thermomechanical storage modulus and relaxation time of SMPs are also critical for the multi-SME. In the progress of phase transition, the temperature-dependent storage modulus of the *i*th soft segment ($E^i(T)$) is a combination of those frozen and active phases, which can be written as follows [15],

$$E^i(T) = E_f^i(T) \phi_f^i(T) + E_a^i(1 - \phi_f^i(T)) \tag{8}$$

where superscripts f and a represent the frozen and active phases in the *i*th soft segment, respectively.

Here the temperature-dependent storage modulus of the frozen phase can be described using a phenomenological equation [37]:

$$\log E_f^i(T) = \log E_f^i(T_{ref}^i) - \alpha^i(T - T_{ref}^i) \tag{9}$$

where $E_f^i(T_{ref}^i)$ is the storage modulus at the referenced temperature T_{ref}^i and α^i is a constant.

It is assumed that the soft segments are in series connections with each other, and parameter λ^i is used to represent the dimensionless length of the *i*th soft segment. Therefore, the overall storage modulus $E(T)$ can be obtained:

$$E(T) = \sum_{i=1}^{n} \lambda^i E^i(T) = \sum_{i=1}^{n} \lambda^i \cdot \left(E_f^i(T)\phi_f^i(T) + E_a^i(1-\phi_f^i(T)) \right) \tag{10}$$

Furthermore, based on the Kohlrausch-Williams Watts (KWW) equation [38,39], the stress decay function $1-\phi^i(t)$ is used to present the remaining fraction of the frozen phase in the *i*th soft segment within the temperature range [T, T+dT], e.g.:

$$1\text{-}\phi^i(t) = 1\text{-}\exp(-(t/\tau^i(T))^{\beta^i}) \tag{11}$$

where $\tau^i(T)$ is the relaxation time and β^i is a given constant. The temperature-dependent relaxation time can be further expressed as [40]:

$$\tau^i(T) = \tau_r^i \exp(\theta(T_r^i - T)) \tag{12}$$

where τ_r^i is the reference of relaxation time and T_r^i is the arbitrary reference of temperature for the *i*th soft segment. Combining Equations (11) and (12), a constitutive relationship of the stress decay function $1-\phi^i(t)$ as functions of relaxation time and temperature can now be obtained, e.g.,

$$1\text{-}\phi^i(t) = 1\text{-}\exp\left\{-\left[t/(\tau_r^i \exp(\theta(T_r^i - T))\right]^{\beta^i}\right\} \tag{13}$$

According to the well-established "thermorheological simplicity" principle [41], the above equation of the relaxation time can be divided into two parts, e.g., the glassy non-equilibrium one and the rubbery non-equilibrium one. Accordingly, the relaxation time can now be expressed as:

$$\tau^i(T) = \tau^i_{g0}\alpha^i(T) \quad \text{(Glassy non-equilibrium condition)} \tag{14a}$$

$$\tau^i(T) = \tau^i_{r0}\alpha^i(T) \quad \text{(Rubbery non-equilibrium condition)} \tag{14b}$$

where $\alpha^i(T)$ is the time-temperature superposition shift factor; τ^i_{g0} and τ^i_{r0} are the relaxation times of the glassy and rubbery states for the *i*th soft segment, respectively, where $\alpha^i(T) = 1$.

As is previously reported [42,43], the time-temperature superposition shift factor can be described using the Williams-Landel-Ferry (WLF) equation, when the polymer is in the rubbery state, e.g.:

$$\log \alpha^i(T) = -\frac{C^i_1(T - T^i_m)}{C^i_2 + (T - T^i_m)} \tag{15}$$

where T^i_m is the WLF referenced temperature for the *i*th soft segment; and C^i_1 and C^i_2 are the material constants for the *i*th soft segment. On the other hand, the time-temperature superposition shift factor is governed by the Arrhenius equation [24], when the polymer in the glassy state, e.g.:

$$\alpha^i(T) = \exp\left(-\frac{A^i F^i_c}{k_b}(T^{-1} - T_g^{i-1})\right) \tag{16}$$

where A^i and F^i_c are constants for the *i*th soft segment, and T^i_g is the corresponding glass transition temperature.

If the polymer is heated at a constant heating rate, the temperature can be expressed

as:

$$T = T_0 + qt \tag{17}$$

where q is the heating rate.

The stress volume function of the frozen phase in the *i*th soft segment can be obtained using the following equation:

$$\begin{aligned}\phi_f^i(t) &= 1+\int_o^t \left[\frac{\partial \phi_f^i(qs+T_0)}{\partial s}(1-\phi^i(t-s)) \right] ds \\ &= 1-\int_o^t \left[qm^i n^i \left[1-\left(\frac{T_0+qs-T_{\min}^i}{T_{\max}^i-T_{\min}^i} \right)^{m^i} \right]^{n^i-1} \cdot \left(\frac{T_0+qs-T_{\min}^i}{T_{\max}^i-T_{\min}^i} \right)^{m^i-1} \cdot (1-\phi^i(t-s)) \right] ds\end{aligned} \tag{18}$$

where term of $\partial \phi_f^i(qs+T_0)/\partial s$ is the volume fraction of the frozen phase which should be unfreezing within the temperature range of $[T_0+qs,\ T_0+q(s+ds)]$. The term of $(1-\phi^i(t-s))$ is the fraction function of the amount $\partial \phi_f^i(qs+T_0)/\partial s$ at *t* (in a unit of minute).

In combination of Equations (7) and (18), the stored strain can finally be obtained,

$$\varepsilon(t) = \sum_{i=1}^{n} \phi_f^i(t)\varepsilon_{pre}^i \tag{19}$$

3. Thermomechanical and shape recovery behavior

Both the thermomechanical properties and shape memory behaviors of the SMPs are originated from their phase transitions and stress relaxations. Generally, dynamic mechanical analysis (DMA) measurements are used to experimentally characterize the thermomechanical properties of SMPs. According to Equation (8), the analytical results of storage modulus have been plotted as a function of temperature to compare with

those obtained in the experimental works reported in Ref. [23]. The results are presented in Fig. 1.

The Universal Global Algorithm (UGO) method is adopted here in order to determine the value of parameters. The convergence tolerance is set as 1×10^{-10} and the maximum iteration is set as 1000. Equation (19) is used to compare with the free recovery behavior of SMPs in order to determine the value of parameters m, n, A, B, τ_r, θ, $T_r - T_0$ and β. Then equation (8) is used to obtain the results and compare with DMA results in order to determine the values of parameters α, T_{ref}, $E_f(T_{ref})$ and E_a. The obtained parameters are used for material calibration. The free recovery behaviors at different heating rates for the same material are then used for the verification of the applicability of the developed model.

The parameters used in Equations (8) and (19) are listed in Table 1. The storage moduli of the SMPs were measured in the temperature range from 310 K to 355 K, using the different heating rates of 1 K/min, 2 K/min and 5 K/min. Simulation results reveal that the storage modulus is gradually increased from 1989 MPa to 1508 MPa with an increase in the heating rate from 1 K/min to 5 K/min. This results in the increase of $T_{\max}$ values from 337.9 K to 352.67 K according to Equation (2). With a large volume fraction of the frozen phase in the SMP, large values of $T_{\max}$ and storage moduli are therefore obtained. This is based on the assumptions that the modulus of frozen phase is always higher than that of the active phase according to Equation (8).

Table 1. Values of parameters used in Equations (8), (9) and (19) for the SMP.

$\phi_f(T)$	$T_{\max}(K)$	$\phi(t)$

m	n	$T_{\min}(K)$	$A(K)$	B(min)	τ_r(min)	$\theta(K^{-1})$	$T_r - T_0(K)$	β
3.50	3.77	311.69	337.9	9.18	$4.2\text{x}10^4$	10^{-5}	3.62	0.35

$E_f(T)$ (MPa)					E_a (MPa)
α	$T_{ref}(K)$	$E_f(T_{ref})$ $(q=1K/\min)$	$E_f(T_{ref})$ $(q=2K/\min)$	$E_f(T_{ref})$ $(q=5K/\min)$	15
0.021	297.34	3000	3465	3968	

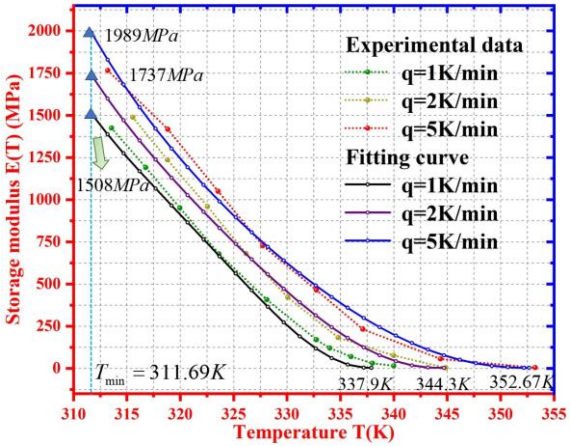

Fig. 1. Comparisons of storage moduli between the experimental data [23] and simulation results using Equation (8), where the heating rates are 1 K/min, 2 K/min and 5 K/min.

On the other hand, recovery strain is another essential property to characterize the SME in SMP. Here, the experimental data of the recovery strains reported in Ref. [23] have been employed for verification of our newly proposed model. The constants used in the Equation (7) are listed in Table 1. Figs. 2(a) and 2(b) present the simulation curves of recovery strains as functions of temperature and relaxation time, respectively, where the heating rates are 1 K/min, 2 K/min and 5 K/min. As shown in Fig. 2(a), the SMP regains its original shape as the $T_{\max}$ is increased from 337.9 K to 352.7 K and the heating rate is increased from 1 K/min to 5 K/min. As presented in Equation (7), the

volume fraction of the soft segment is gradually increased with an increase in the heating rate, thus resulting in a large recovery strain. The simulation results reveal that the values of T_{max} is increased with the increase of the heating rate, thus resulting in a full recovery of strain at a high temperature. Meanwhile, the relaxation time is also increased from 8.2 min to 26.3 min with the increase in the heating rate, as revealed in Fig. 2(b). It is found that the simulation results obtained from our model fit well with the experimental data, and the shape recovery behavior of the SMP has been well described using this new model.

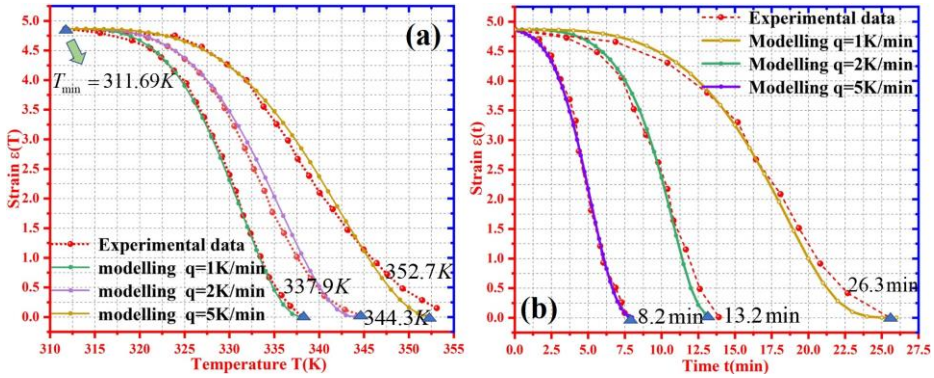

Fig. 2. Comparisons of shape recovery behaviors between the experimental data [23] and simulation results using Equation (7), where the heating rates are 1 K/min, 2 K/min and 5 K/min. (a) the recovery strain as a function of temperature. (b)the recovery strain as a function of time.

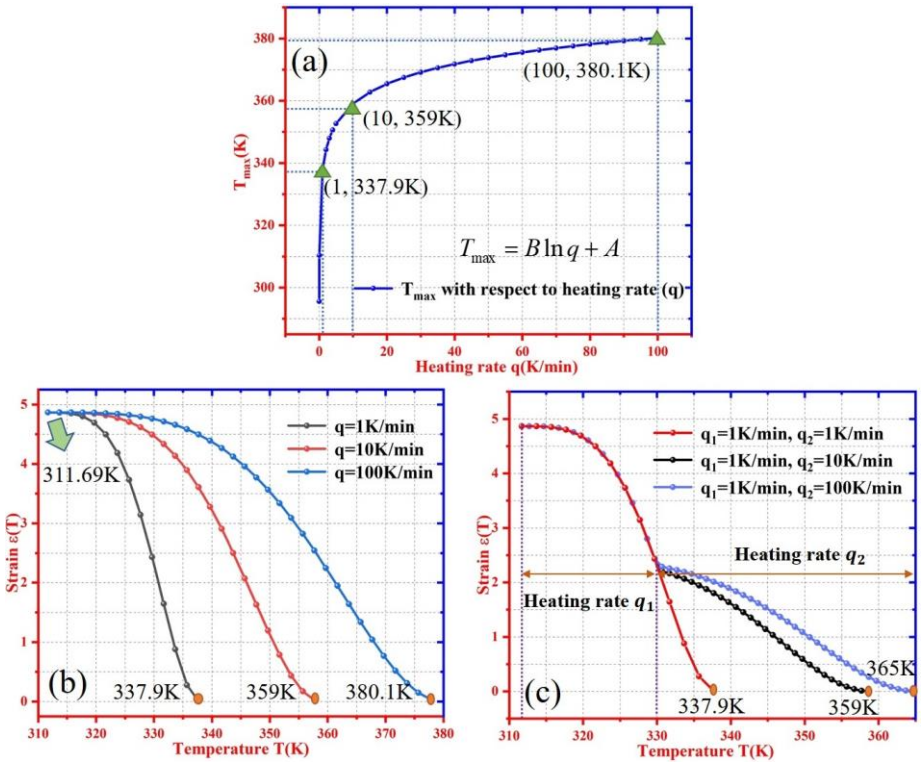

Fig. 3. (a) T_{max} with respect to heating rate. (b) One-stage recovery strain as a function of temperature at the heating rates of q=1 K/min, 10 K/min and 100 K/min. (c) Two-stage recovery strains as a function of temperature at the two stage heating, with first stage heating rate q_1=1 K/min, while the second stage heating rate q_2=1K/min, 10K/min and 100K/min.

To further investigate the effect of heating rate, a shape recovery behavior of the SMP which is actuated at two different heating rates has been considered. Fig. 3(a) plots the simulation curve of T_{max} as a function of heating rate increased from 0.01 K/min to 100 K/min. It is revealed that the value of T_{max} is increased from 337.9 K to 380.1 K with an increase of the heating rate from 1 K/min to 100 K/min. The effect of the heating rate on the recovery strain of the SMP is plotted in Fig. 3(b) and Fig. 3(c), which shows the simulated recovery strains are increased with an increase in the heating rate as a function of temperature. Furthermore, a two-stage recovery strain was also obtained if

using two-step heating rates, where q_1=1K/min is used in the first step, and q_2=1 K/min, 10 K/min or 100 K/min are used in the second one. Simulation results show that the recovery strain is significantly influenced by the heating rate. In the second stage, the $T_{\max}$ is gradually increased from 337.9 K to 380.1 K with an increase in the heating rate from q_2=1 K/min to q_2=100 K/min. These simulation results prove that two-stage or multi-stage recovery strain can be designed and achieved by using different heating rates.

Fig. 1 and Fig. 2 show the comparisons between the experimental data of the storage moduli and recovery strains, which have been used for the calibration. Based on the parameters listed in Table 1, we investigated the free recovery process of the stored strain of the same material at variable heating rates. The results are shown in Fig. 4, which can be used for the verification of the applicability of our model. The results shown in Fig. 4 are more accurately to describe the complicated recovery and stress relaxation behavior in SMPs, if compared with the results obtained using the previously proposed model in literature [23]. Due to the structural decay arrangement in the amorphous polymers, , the relaxation duration of the SMP is increased, and the stored strain within the same temperature interval (5K) are increased, when the heating rate is low. Meanwhile, the number of the parameters which are needed in this newly proposed model is 15. This is far less than 77 parameters needed in the previously proposed model [23] which significantly reduces complexity of the computation.

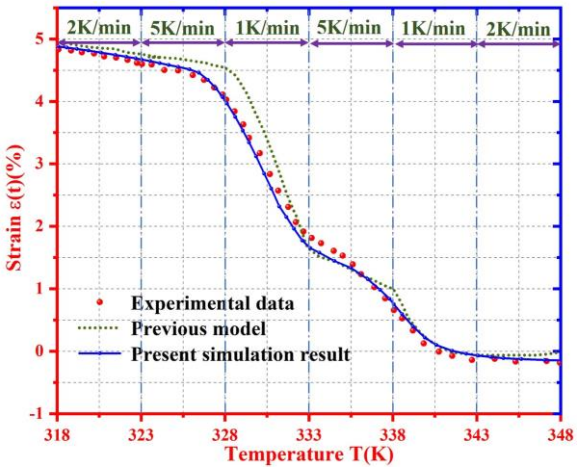

Fig. 4. Comparisons of shape recovery behaviors among the experimental data [23], simulation results using Equation (19), results obtained using the previously porposed model [23] at various heating rates of 1 K/min, 2 K/min and 5 K/min.

4. Cooperative dynamics

For the multi-SME in SMP, it is normally required that there are more than three segments involved in the stress relaxation processes. At the same time, more than two soft segments will need to undergo glass transitions. However, experimental work is difficult to reveal the cooperative dynamics in multiple glass transitions and stress relaxations of the SMP. Therefore, it is necessary to theoretically explore the cooperative dynamics of the SMP with multi-SME.

Experimental data of storage modulus and recovery strain published in Ref. [30] have been used here to investigate the thermomechanical and shape recovery behaviors of the SMP which undergoes two-stage glass transitions and stress relaxations. The simulated results of storage modulus and recovery strain of the SMP have been plotted in in Fig. 5(a) and Fig. 5(b), respectively, to compare with the experimental data [30].

The constants and parameters used in the Equations (7) and (10) are listed in Table 2. It is found that the simulation results of storage moduli of the SMPs fit well with the experimental data as shown in Fig. 5(a). The SMP undergoes two-stage glass transitions, where the first one occurs in the temperature range from $T_{\min}^{1}$=297 K to $T_{\max}^{1}$=333 K, whereas the second one occurs in a range from $T_{\min}^{2}$=325 K to $T_{\max}^{2}$=363 K. Meanwhile, it should be pointed out that there is a strong coupling effect of two soft segments due to the superposition of the transition temperatures. This is because the full transition temperature ($T_{\max}^{1}$=333 K) of the first soft segment is higher than that of the $T_{\min}^{2}$=325 K of the following second soft segment.

Table 2. Values of parameters used for the SMP with two-stage glass transitions and stress relaxations.

Parameter	The first transition phase	The second transition phase
λ	0.559	0.441
$E_f(MPa)$	1148.07	142.5
$E_a(MPa)$	10	7.19
m	1.84	1.89
n	3.77	4.75
$T_{\min}(K)$	297	325
$T_{\max}(K)$	333	363
$\tau_{g0}(\min)$	2.287	6.54
$\tau_{r0}(\min)$	10^{-6}	0.009
C_1	10	5

C_2	30	51
T_m (K)	353.38	413
ε_{pre}	0.0172	0.031

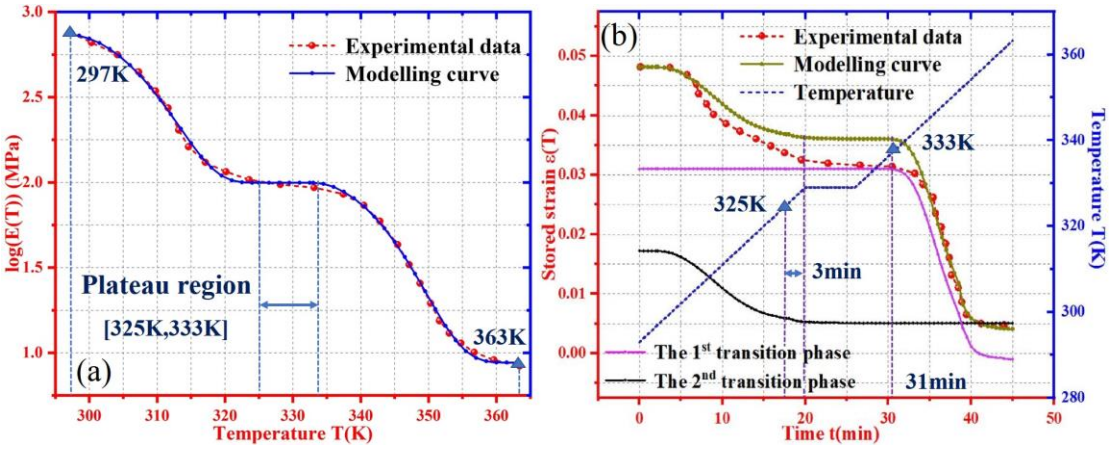

Fig. 5. (a) Comparisons of storage moduli as a function of temperature between the experimental data [30] and simulation results using Equation (10). (b) Comparisons of stored strains as a function of relaxation time between the experimental data [30] and simulation results using Equation (7).

On the other hand, the simulation results of time-dependent recovery strains of the SMPs are also plotted in Fig. 5(b), and then compared with the experimental results [30]. It is found the stored strain is gradually decreased from 4.8% to 0% with an increase in relaxation time from 0 min to 45 min. In the initial transition temperature range from 297 K to 333 K, the stored strain in the SMP is released with an increase in the temperature and relaxation time. The SMP took ~31 min to complete the transition process at the full transition temperature of $T^1_{\max}$ =333 K. Whereas the following glass transition of the second soft segment is induced at the initial transition temperature of

$T^2_{\min}$ =325 K. It took ~28 min to complete the transition process when it was heated to $T^2_{\max}$ =363 K. Furthermore, there is a cooperative relaxation of two soft segments in the time range from 17 min to 31 min. That is to say, the recovery strain is determined by the cooperative relaxations of two soft segments in the temperature range from 325 K to 333 K. These numerical results are in well agreements with the experimental data reported in Ref. [30]. A two-stage glass transition porcess and stress relaxations in the SMP have well characterized and predicted using our newly proposed model.

If the cooperative relaxation is not clearly presented due to the overlapping of two stress relaxation stages, it is necessary to characterize this two-stage glass transition at the molecular scale. Here the experimental data of Nafion SMPs reported in Ref. [31] have been employed to compare with the simulation results obtained using our proposed model, both of which are shown in Fig. 6. The constants used in the Equations (7) and (19) are listed in Table 3.

Table 3. Values of parameters used for the Nafion SMP with multi-SME.

1st transition phase	A^1 (K)	B^1 (min)	$T^1_{\min}$ (K)	ε^1_{pre}	q(K/min)	m^1	n^1
	347.66	3.37	293	0.036	0.5	6.56	14.05
					1	4.35	3.39
					5	3.77	6.82
2nd transition phase	A^2 (K)	B^2 (min)	$T^2_{\min}$ (K)	ε^2_{pre}	q(K/min)	m^2	n^2
	390.76	13.85	330	0.045	0.5	1.59	1.92
					1	2.78	7.87
					5	1.93	3.84

As revealed in Fig. 6(a), Fig. 5(c) and Fig. 5(e), the recovery strains of SMP were successfully obtained at different heating rates of 0.5 K/min, 1 K/min and 5 K/min,

respectively. According to these experimental data [31] and simulation results, only one-stage glass transition process is observed in the strain recovery process. Whereas we know that there should have two glass transitions of two soft segments in the SMP. The reason why these two glass transitions have not been shown is mainly attributed to the cooperative effect of two soft segments in the SMPs.

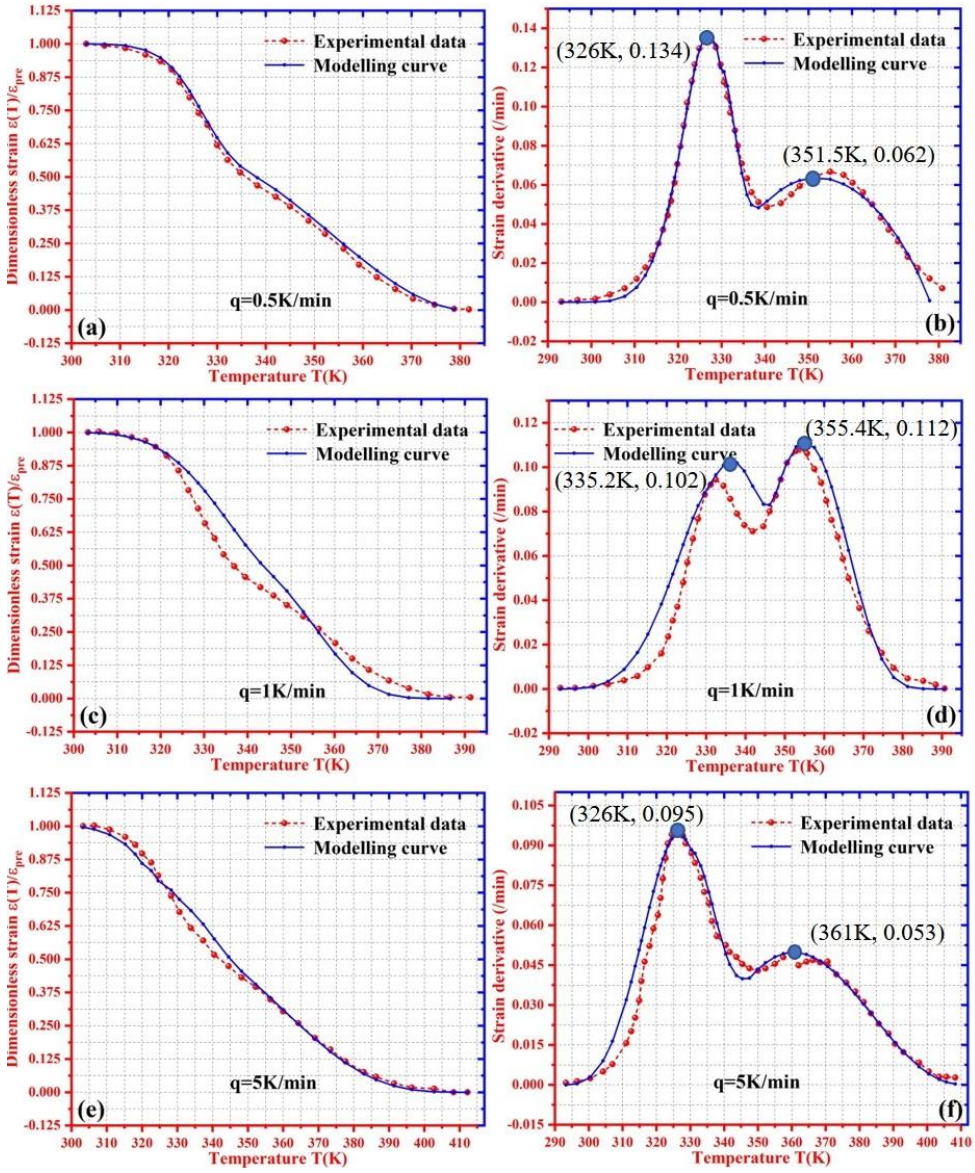

Fig. 6. (a), (c), (e). Recovery strains of SMP as a function temperature at a heating rate of 0.5 K/min, 1 K/min and 5 K/min, respectively. (b), (d), (f). First-order derivative curves of recovery strains as a function temperature at a heating rate of 0.5 K/min, 1

K/min and 5 K/min, respectively.

To reveal more detailed kinetics information, the first-order derivative of recovery strain of the Nafion SMP was calculated and are plotted in Fig. 6(b), Fig. 6(d) and Fig. 6(f), at the different heating rates of 0.5 K/min, 1 K/min and 5 K/min, respectively. The experimental and simulation curves all show a similar pattern consisting of two opposite peaks. The glass transition temperatures can be determined by analyzing the corresponding peak values of the recovery strain curves shown in Fig. 6(a), Fig. 6(c) and Fig. 6(e). Based on these simulation results, there are two transition temperatures identified, i.e., (T_g^1=326 K, T_g^2=351.5 K), (T_g^1=335.2 K, T_g^2=355.4 K) and (T_g^1=326 K, T_g^2 =361 K), respectively. However, it should be noted that the peaks are significantly determined by the cooperative dynamics in the two-stage glass transition processes. This has resulted in shifts of the peak values and their amplitudes at different heating rates.

To further verify the coupling interactions, dependence of cooperative dynamics on the full transition temperature ($T_{\max}$) of the soft segment has been investigated. The results are expected to reveal the coupling interaction between two soft segments and cooperative dynamics in the multi-stage glass transitions. The effect of $T_{\max}$ of the first soft segment on the recovery strain has been plotted in Fig. 7. All the used constants are listed in Table 3. As shown in Fig. 7(a) and Fig. 7(b), the obtained stored strains and first-order derivative strains are presented as a function of temperature at a constant heating rate of q=0.5 K/min. The peak position obtained from the derivative strain

curves of Fig. 7(b) is defined as the T_g value of the soft segments. It is found that the T_g^1 is gradually shifted from 313 K to 335 K when the $T_{\max}^1$ is increased from 325 K to 355 K. While the $T_{\min}^2$ of second soft segment has been kept a constant. Simulation results clearly show that the coupling interaction is determined by the cooperative effect of $T_{\max}^1$ and $T_{\min}^2$. With a decrease in the difference in T_g^1 and T_g^2 from 55 K to 25 K, the typical two-stage glass transition processes are not presented in the recovery strain curve due to a strong cooperative effect.

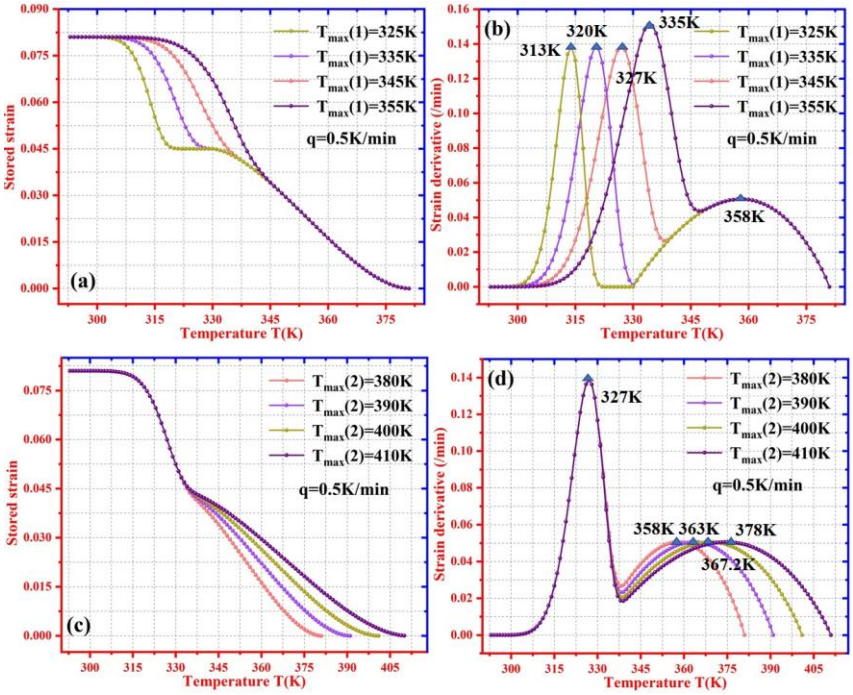

Fig. 7. (a). Simulation results of the stored strains as a function of temperature, while the $T_{\max}^1$ is increased from 325 *K*, 335 *K*, 345 *K* to 355 *K*. (b) First-order derivative curves of stored strains with $T_{\max}^1$=325 *K*, 335 *K*, 345 *K* and 355 *K*. (c). Simulation results of the stored strains as a function of temperature, while the $T_{\max}^2$ is increased from 380 *K*, 390 *K*, 400 *K* to 410 *K*. (d) First-order derivative curves of stored strains with $T_{\max}^2$=380 *K*, 390 *K*, 400 *K* and 410 *K*.

On the other hand, the effect of $T_{\max}^2$ on the coupling interaction of two soft segments has further been investigated. Fig. 6(c) and Fig. 6(d) show the simulation results of stored strain and first-order derivative strains of the SMPfor the cases of $T_{\max}^2$ =380 K, 390 K, 400 K, 410 K and a heating rate of 0.5 K/min. Simulation results clearly show that the T_g^2 is gradually increased from 358 K to 378 K when the $T_{\max}^2$ is increased from 380 K to 410 K. The coupling interaction of two transitions is also determined by the $T_{\max}^2$.

Based on these simulation results, the two-stage recovery strain is strong determined by the thermomechanical properties of the soft segments in SMP. Furthermore, a cooperative dynamic is presented between these soft segments due to their simultaneously relaxations. A strong cooperative effect makes it difficult to show a clear two-stage relaxation as revealed by the simulation results. Here, the cooperative dynamics in two-stage glass transitions is then similar to that in the SMP with multi-SME.

5. Conclusion

In this study, a one-dimensional coupling model was proposed to describe the multiple glass transitions and their thermomechanical behaviors of the SMPs with multi-SME. The segmental relaxations of multiple soft segments have been identified as the driving force for multi-SME and the overall relaxation behavior is formulated by the Boltzmann's superposition principle. The cooperative dynamics of multi-SME has been characterized and verified by the simulation and experimental results. Dependence

of the coupling interaction on the full transition temperature (T_{max}) and initial transition temperature (T_{min}) of soft segments has been investigated. The constitutive relationships among storage modulus, recovery strain, first-order derivative strain, relaxation time and heating rate of the SMP have been theoretically investigated and discussed. Finally, the simulation results were compared and verified by the experimental data reported in the literature, and good agreements between the theoretical and experimental results had been achieved. This study is expected to provide a theoretical guidance to understand and design of multi-SME in SMPs.

Acknowledgements

This work was financially supported by the National Natural Science Foundation of China (NSFC) under Grant No. 11672342 and 11725208, Newton Mobility Grant (IE161019) through Royal Society and NFSC.

References

[1] P.T. Mather, X.F. Luo, I.A. Rousseau, Shape memory polymer research, Annu. Rev. Mater. Res. 39 (2009) 445-471.

[2] H.B. Lu, Y.T. Yao, W.M. Huang, D Hui, Noncovalently functionalized carbon fiber by grafted self-assembled graphene oxide and the synergistic effect on polymeric shape memory nanocomposites, Compos. B. Eng. 67 (2014) 290-295.

[3] A. Lendlein, H. Jiang, O. Junger, R. Langer, Light-induced shape-memory polymers, Nature 434 (2005) 879-882.

[4] R. Mohr, K. Kratz, T. Weigel, G.M. Lucka, M. Moneke, A. Lendlein, Initiation of shape-memory effect by inductive heating of magnetic nanoparticles in thermoplastic polymers, Proc. Natl. Acad. Sci. USA 103 (2006) 3540-3545.

[5] K. Hilmar, K.P. Gary, A.P. Nathan, A. Max, A.V. Richard, Remotely actuated polymer nanocomposites—stress-recovery of carbon-nanotube-filled thermoplastic elastomers, Nature Mater. 3 (2004) 115-120.

[6] C.M. Yakacki, R. Shas, C. Lanning, B. Rech, A. Eckstein, K. Gall, Unconstrained recovery characterization of shape-memory polymer networks for cardiovascular applications, Biomaterials 28 (2007) 2255-2263.

[7] A. Lendlein, S. Kelch, Shape-memory polymers as stimuli-sensitive implant materials, Clin. Hemorheol. Microcirc. 32 (2005) 105.

[8] Y.P. Liu, K. Gall, M.L. Dunn, P.M. Cluskey, Thermomechanics of shape memory polymer nanocomposites, Mech. Mater. 36 (2004) 929-940.

[9] H. Tobushi, H. Hara, E. Yamada, S. Hayashi, Thermomechanical properties in a thin film of shape memory polymer of polyurethane series, Smart Mater. Struct. 5 (1996) 483-491.

[10] Q. Meng, J. Hu, A review of shape memory polymer composites and blends,

Compos. Part A Appl. Sci. Manuf. 40 (2009) 1661-1672.

[11] M. Behl, A.J. Lendlein, Triple-shape polymers, Mater. Chem. 20 (2010) 3335-3345.

[12] I.S. Kolesov, H.J. Radusch, Multiple shape-memory behavior and thermal-mechanical properties of peroxide cross-linked blends of linear and short-chain branched polyethylenes, Express Polym. Lett. 2 (2008) 461-473.

[13] X. Luo, P.T. Mather, Triple-Shape Polymeric Composites (TSPCs), Adv. Funct. Mater. 20 (2010) 2649-2656.

[14] A. Heuer, M. Wilhelm, H. Zimmermann, H.W. Spiess, Rate memory of structural relaxation in glasses and its detection by multidimensional NMR, Phys. Rev. Lett. 75 (1995) 2851-2854.

[15] Y. Liu, K. Gall, M.L. Dunn, A.R. Greenberg, J. Diani, Thermomechanics of shape memory polymers: Uniaxial experiments and constitutive modeling, Int. J. Plast. 22 (2006) 279-313.

[16] H. Lu, X. Wang, Y. Yao, Y. Fu, A “frozen volume” transition model and working mechanism for the shape memory effect in amorphous polymers, Smart Mater. Struct. 27 (2018) 065023.

[17] Y. Li, J. Hu, Z. Liu, A constitutive model of shape memory polymers based on glass transition and the concept of frozen strain release rate, Int. J. Solids Struct. 7683 (2017) 30311-30316.

[18] Q. Yang, G, Li, Temperature and rate dependent thermomechanical modeling of shape memory polymers with physics based phase evolution law, Int. J. Plasticity

80 (2015) 168-186.

[19] P. Gilormini, J. Diani, On modeling shape memory polymers as thermoelastic two-phase composite materials, Comptes Rendus Mécanique 340 (2012) 4-5.

[20] S. Reese, M. Böl, D. Christ, Finite element-based multi-phase modelling of shape memory polymer stents, Comput. Method. Appl. M. 199 (2010) 1276-1286.

[21] C. Fang, J. Leng, H. Sun, J. Gu, A multi-branch thermoviscoelastic model based on fractional derivatives for free recovery behaviors of shape memory polymers, 2018 Mech. Mater. 120 (2018) 34-42.

[22] Q. Ge, K. Yu, Y. Ding, H.J. Qi, Prediction of temperature-dependent free recovery behaviors of amorphous shape memory polymers, Soft Matter 8 (2012) 11098.

[23] M. Lei, K. Yu, H. Lu, H.J. Qi, Influence of structural relaxation on thermomechanical and shape memory performances of amorphous polymers, Polymer 109 (2017) 216-228.

[24] K. Yu, T. Xie, J. Leng, Y. Ding, H.J. Qi, Mechanisms of multi-shape memory effects and associated energy release in shape memory polymers, Soft Matter 8 (2012) 5687.

[25] F. Castro, K. K. Westbrook, K. N. Long, R. Shas, H. J. Qi, Effects of thermal rates on the thermomechanical behaviors of amorphous shape memory polymers, Mech. Time-Dependent Mater. 14 (2010) 219-241.

[26] I. Bellin, S. Kelch, R. Langer, A. Lendlein, Polymeric Triple-Shape Materials, Proc. Natl. Acad. Sci. USA 103 (2006) 18043-18047.

[27] T. Pretsch, Triple-shape properties of a thermoresponsive poly(ester urethane),

Smart Mater. Struct. 19 (2010) 015006.

[28] G. Hu, A.R. Damanpack, M. Bodaghi, W.H. Liao, Increasing dimension of structures by 4D printing shape memory polymers via fused deposition modeling, Smart Mater. Struct. 26 (2017) 125023.

[29] M. Bodaghi, A.R. Damanpack, W.H. Liao, Adaptive metamaterials by functionally graded 4D printing, Mater. Des. 135 (2017) 26–36.

[30] T. Xie, X. Xiao, Y. T. Cheng, Revealing Triple-Shape Memory Effect by Polymer Bilayers, Macromol. Rapid Commun. 30 (2009) 1823-1827.

[31] J. Li, T. Xie, Significant Impact of Thermo-Mechanical Conditions on Polymer Triple-Shape Memory Effect, Macromolecules 44 (2011) 175-180.

[32] Y. Li, Z. Liu, A novel constitutive model of shape memory polymers combining phase transition and viscoelasticity, Polymer 143 (2018) 298–308.

[33] M. Bodaghi, A.R. Damanpack, W.H. Liao, Triple shape memory polymers by 4D printing, Smart Mater. Struct. 27 (2018) 065010.

[34] H. Lu, X. Wang, K. Yu, Y. Fu, J. Leng, A phenomenological formulation for the shape/temperature memory effect in amorphous polymers with multi-stress components, Smart Mater. Struct. 28 (2019) 025031.

[35] X. Wang, H. Lu, X. Shi, K. Yu, Y. Fu, A thermomechanical model of multi-shape memory effect for amorphous polymer with tunable segment compositions, Compos. Part B Eng. 160 (2019) 298-305.

[36] A.J. Kovacs, J.M. Hutchinson, Isobaric thermal behavior of glasses during uniform cooling and heating: Dependence of the characteristic temperatures on the relative

contributions of temperature and structure to the rate of recovery. II. A one-parameter model approach, J. Polym. Sci. Pol. Chem. 17 (1979) 2031-2058.

[37] E.M. Arruda, M.C. Boyce, Evolution of plastic anisotropy in amorphous polymers during finite straining, Int. J. Plast. 9 (1993) 697-720.

[38] M. L. Mansfield, Model of the glass transition, J. Chem. Phys. 103 (1995) 8124–8129.

[39] G. Williams, D.C. Watts, Molecular motion in the glassy state. The effect of temperature and pressure on the dielectric β relaxation of polyvinyl chloride, Trans. Faraday Soc. 67 (1971).

[40] C.T. Moynihan, A.J. Easteal, J. Wilder, J. Tucker, Dependence of the glass transition temperature on heating and cooling rate, J. Phys. Chem. 78 (1974) 2673-2677.

[41] O.S. Narayanaswamy, Thermorheological simplicity in the glass transition, J. Am. Ceram. Soc. 71 (1988) 900–904.

[42] P. A. O'Connell, G. B. McKenna, Arrhenius-type temperature dependence of the segmental relaxation below T_g, J. Chem. Phys. 110 (1999) 11054.

[43] M. L. Williams, R. F. Lel, J. D. Ferry, The temperature fependence of relaxation mechanisms in amorphous polymers and other glass-forming liquids, J. Am. Chem. Soc. 77 (1955) 3701-3707.

Tables caption

Table 1. Value of parameters used in Equations (9) (10) and (20) for the SMP.

Table 2. Value of parameters used for the SMP with two-stage glass transitions and structural relaxations.

Table 3. Value of parameters used for the Nafion SMP with multi-SME.

Figures caption

Fig. 1. Comparison of storage modulus between the experimental data [23] and simulation results using Equation (9), where the heating rates are 1K/min, 2K/min and 5K/min.

Fig. 2. Comparison of shape recovery behavior between the experimental data [23] and simulation results using Equation (8), where the heating rates are 1K/min, 2K/min and 5K/min. (a). For the recovery strain as a function of temperature. (b). For the recovery strain as a function of time.

Fig. 3. (a) $T_{\max}$ with respect to heating rate. (b) One-stage recovery strain as a function of temperature at the heating rate q=1K/min, 10K/min and 100K/min. (c) Two-stage recovery strain as a function of temperature at the heating rate q_1=1K/min, while q_2 =1K/min, 10K/min and 100K/min.

Fig. 4. Comparison of shape recovery behavior among the experimental data [23], simulation results using Equation (19), previous model results [23] at various heating rate 1K/min, 2K/min, and 5K/min.

Fig. 5. (a) Comparison of storage modulus as a function of temperature between the experimental data [31] and simulation results using Equation (11). (b) Comparison of stored strain as a function of relaxation time between the experimental data [31] and simulation results using Equation (8).

Fig. 6. (a), (c), (e). Recovery strain of SMP as a function temperature at a heating rate of 0.5 K/min, 1 K/min and 5 K/min, respectively. (b), (d), (f). First-order derivative curves of recovery strain as a function temperature at a heating rate of 0.5 K/min, 1 K/min and 5 K/min, respectively.

Fig. 7. (a). Simulation results of the stored strains as a function of temperature, while the $T_{\max}^{1}$ is increased from 325 *K*, 335 *K*, 345 *K* to 355 *K*. (b) First-order derivative curves of stored strains with $T_{\max}^{1}$=325 *K*, 335 *K*, 345 *K* and 355 *K*. (c). Simulation results of the stored strains as a function of temperature, while the $T_{\max}^{2}$ is increased from 380 *K*, 390 *K*, 400 *K* to 410 *K*. (d) First-order derivative curves of stored strains with $T_{\max}^{2}$=380 *K*, 390 *K*, 400 *K* and 410 *K*.